

# 3D RECONSTRUCTION OF THE SPINE FROM UNCALIBRATED BIPLANAR INTRA-OPERATIVE X-RAY IMAGES

Justin Novosad<sup>1,2</sup>, Farida Cheriet<sup>1,2</sup>, Hubert Labelle<sup>2</sup>

<sup>1</sup> École Polytechnique, Montréal, Québec, Canada

<sup>2</sup> Sainte-Justine Hospital Research Centre, Montréal, Québec, Canada

## ABSTRACT

A new technique for the intra-operative 3D reconstruction of the spine from biplanar chest radiographs was developed. The technique uses a self-calibration algorithm that does not require a calibration object; the radiographic set-up is calibrated from the natural content of the images (i.e. matched anatomical landmarks and surgical implants). Since no calibration object is required, the technique is suitable for the retrospective study of scoliosis surgical treatments in 3D.

An automatic procedure for the selection of matched landmarks was implemented in order to improve the quality of the results. This algorithm selects a subset of the available landmarks that are to be used for the calibration procedure. The selection criteria are based on quality of stereo-correspondence and breadth of spatial distribution.

In vitro and in vivo tests showed that the proposed technique is feasible and reaches the expected accuracy.

## INTRODUCTION

In the past decade, many clinical studies have used three-dimensional data for the evaluation of spinal deformities. Three-dimensional reconstruction from bi-planar radiographs exposes the patient to a much safer dose of ionizing radiation than x-ray computerized tomography (CT), and is much more cost effective than magnetic resonance imaging (MRI). Once the patient has been treated using steel surgical implants, MRI is no longer an option and CT scans produce poor images because of ringing artifacts. Furthermore, MRI and CT are not as accessible as conventional x-rays. Therefore, bi-planar stereo-radiography is one of the most attractive 3D imaging modalities for the intra-operative 3D reconstruction of the spine. At the present time, the most widely used calibration and reconstruction algorithm for bi-planar radiographs is the Direct Linear Transform (DLT). Previous work defends the accuracy and maturity of this technique [3, 4].

The DLT requires that a large calibration object be placed around the patient when the X-ray images are taken. The calibration object use at Sainte-Justine Hospital consists of two sheets of Plexiglas with incrusted steel pellets. One of the sheets is in front of the standing patient, the other is behind. This calibration object is used for the acquisition of preoperative and postoperative x-rays. It is not suitable for intra-operative x-rays.

To solve this problem, an explicit calibration method was introduced for intra-operative biplanar radiographic systems [1]. The explicit calibration algorithm is based on the nonlinear optimization of a set of geometric parameters that describe the radiographic set-up. It requires only a small calibration object that is conveniently placed over the patient during the acquisition of intra-operative radiographs. The technique is suitable for intra-operative reconstruction; but it cannot be used retrospectively. Retrospective intra-operative 3D reconstruction is required for the comparative study of current surgical techniques against older procedures. Furthermore, the elimination of the intra-operative calibration object would be an improvement, since it would eliminate the need for additional steps in a surgical procedure that is complex enough as it is.

The self-calibration procedure proposed in this paper uses only the natural content of the images (anatomical landmarks, surgical implants, etc.). From this information alone, it is possible to estimate the parameters that describe the radiographic set-up.

Self-calibration in the intra-operative context is somewhat challenging because of high pose variability and poor image quality (compared to preoperative and postoperative). The anatomical landmarks are manually matched on both views by an expert. Thus the matches are subject to human error. This problem has prompted the introduction of an important algorithm enhancement that is presented in this paper: automatic calibration landmark selection. The idea is to select a high quality subset of all the available stereo-corresponding landmarks based on a quality of correspondence criterion and breadth of spatial distribution. Only the selected landmarks are used in the self-calibration process.

## SELF-CALIBRATION

### The Basic Self-Calibration Algorithm

The self-calibration algorithm, just like the explicit calibration algorithm, is based on the minimization of landmark retroprojection errors by optimizing geometric parameters that describe the radiological set-up. These parameters are a 3D translation (position of the x-ray source), a 3D rotation (orientation of the image plane), and perspective projection parameters (principal distances and the principal point). The main difference between self-calibration and explicit calibration is that the real 3D coordinates of the landmarks used for calibration are unknown in the self-calibration context. To overcome this problem, an initial approximation of the geometric parameters is used to generate a 3D reconstruction of the anatomical landmarks. The reconstructed landmarks are then used as a *virtual* calibration object. Using this virtual calibration object, the system can be calibrated using the explicit calibration algorithm as described in [2]. With the geometric parameters resulting from explicit calibration, the virtual calibration object is regenerated. This procedure is repeated until the system reaches a steady state. The algorithm can be expressed as follows:

1. Initialize  $\xi$  with an initial estimation of the geometric parameters.
2. Reconstruct the matched calibration landmarks by stereo triangulation using  $\xi$ . Let  $C$  denote the result of the reconstruction.
3. Perform explicit calibration [2] using  $C$  as the calibration object and using  $\xi$  as the initial approximation. Update  $\xi$  with the result.
4. Repeat steps 2 and 3 until convergence.

### Performance Considerations

Given the relatively high number of geometric parameters (10 per view, 20 in all), the calibration algorithm takes a long time to converge. Two modifications were made in order to improve performance. First of all, two of the geometric parameters are redundant: the x principal distance and the y principal distance. In the general case, these parameters are independent, but in the case where the image aspect ratio is 1, these two parameters are necessarily equal. With scanned intra-operative X-rays, the aspect ratio of the scanner is specified by the manufacturer. This information can be used to correct the image and make its aspect ratio to 1. This trick brings the total number of parameters down to 18.

A second modification of the algorithm involves the partitioning of the parameter space. Instead of optimizing all parameters simultaneously, it is much more computationally efficient to optimize only a subset of the parameters at a time. The parameters were partitioned into three groups: rotation, translation and intrinsic parameters. Looping over the three parameter groups several times yields results as good as simultaneous optimization, in a fraction of the time. This optimization of the algorithm had the total self-calibration execution time drop from several minutes to a few seconds on an Athlon XP1800+ computer (actual execution time varies from one case to another).

### Landmark Selection

The self-calibration algorithm is very sensitive to the quality of the input data that is acquired through an error prone manual process. The uncertainty in the matching of stereo-corresponding landmarks is a critical factor that can determine whether the self-calibration algorithm converges or not. In order to avoid the ill-conditioning of the system, an algorithm was implemented that automatically selects the landmarks that are to be used for the calibration process.

The first selection criterion is based on the distance of a point to its corresponding epipolar line. The line equation coefficients of a point's corresponding epipolar line are given by the product of the corresponding point in the other image by the fundamental matrix. For more information on epipolar lines and the fundamental matrix, the reader should refer to [5]. In the ideal case, stereo-corresponding points are located exactly on their corresponding epipolar lines. A robust estimation of the fundamental matrix is obtained through the improved eight-point algorithm proposed by Hartley [6].

Since the epipolar constraint offers one degree of freedom (point-to-line), it follows that points that respect the constraint are not necessarily perfect matches; however, such matches are necessarily consistent with the stereo projection model, thus they will not hinder the calibration process.

The second selection criterion is spatial distribution. The selected group of landmarks must not be concentrated in the same regions of the two images. The calibration results are much less sensitive to noise when a well dispersed group of landmarks is used. Such a group of points is obtained by maximizing a dispersion function that is expressed as follows:

$$\Phi(p) = \left[ \prod_{i=1}^n \prod_{j=i+1}^n \|p_{i,1} - p_{j,1}\| \cdot \|p_{i,2} - p_{j,2}\| \right]^{\frac{1}{n^2-n}}$$

Where  $p$  is the set of selected landmarks,  $n$  is the cardinality of  $p$ ,  $p_{i,m}$  is the 2D coordinate of the  $i^{\text{th}}$  landmark of  $p$  as measured on image  $m$ . This equation represents a multiplicatively pondered central tendency of inter-point distances.

Here is simple heuristic algorithm that takes into account both selection criteria:

1. Store the set of all matched landmarks in  $P$ .
2. From  $P$ , calculate the fundamental matrix using the improved eight-point algorithm [6].
3. Remove outliers from  $P$ . Outliers are landmarks that are too far from their epipolar lines on one of the images.
4. Let  $p$  be initially empty.
5. Add to  $p$  the landmark  $P_i$  that maximizes  $\chi(P_i)\Phi(p \cup P_i)$ . Where  $\chi(P_i)$  is a function that expresses the degree to which  $P_i$  satisfies the epipolar constraint.
6. Remove the landmark selected in step 5 from  $P$ .
7. Repeat steps 5 and 6 until enough calibration landmarks are selected.

## RESULTS

The reliability of self-calibration was previously validated in vitro and in vivo for the reconstruction of scoliotic spines from post-operative x-rays [8]. The results presented in this paper illustrate that the algorithm, when combined with the landmark selection process, is also suitable for intra-operative reconstruction.

To reconstruct the spine, six anatomical landmarks per vertebra (centers of superior and inferior vertebral endplates and the superior and inferior extremities of both pedicles) were manually identified and matched by an expert. A subset of these landmarks was chosen by the selection algorithm presented earlier. The selected landmarks were used for performing self-calibration. The geometrical parameters resulting from the self-calibration algorithm were used to reconstruct 3D spine models by triangulation [5]. This procedure was performed on five pairs of real biplanar intra-operative X-rays.

The first experiment consisted in analyzing the root-mean-squared retro-projection errors of each spine reconstructed with the self-calibration technique. The experiment was repeated several times using different numbers of landmarks to study the impact of the number of landmarks used for self-calibration on the quality of the output of the self-calibration algorithm. The results of this experiment are shown in Figure 1. The graph shows that quality increases (error decreases) as the number of calibration landmarks increases. It should also be noted that very little is gained by using more than 15 landmarks.

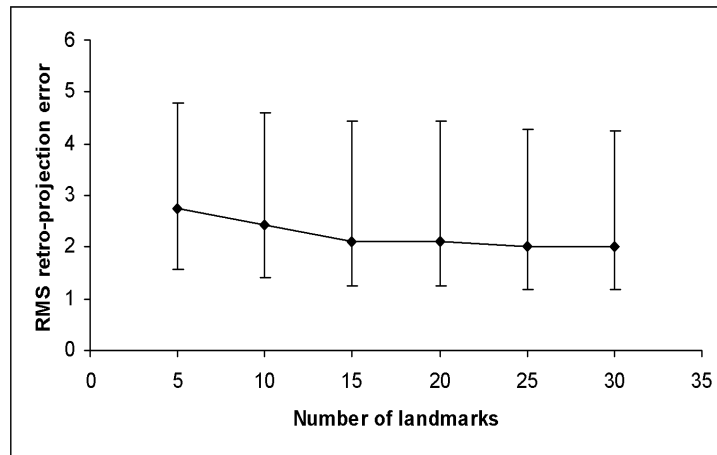


Figure 1: Full specimen RMS retro-projection error in millimeters (average, minimum, maximum) vs. Number of landmarks used for self-calibration

One of the spines was also reconstructed using the explicit calibration algorithm [2] with a small calibration object. The two reconstructions are shown in Figure 2. There is very little visible difference between the graphic representations produced by both techniques. A metric registration between the two models was carried-out in order to uncover the scale and orientation errors induced by the self-calibration procedure. The resulting scale factor was 1.04. The relative rotation about the x, y and z axes were 2.7, 0.8 and  $-3.8$  degrees respectively. After performing the registration, the root-mean-square of distances between corresponding landmarks was 1.12 millimetres.

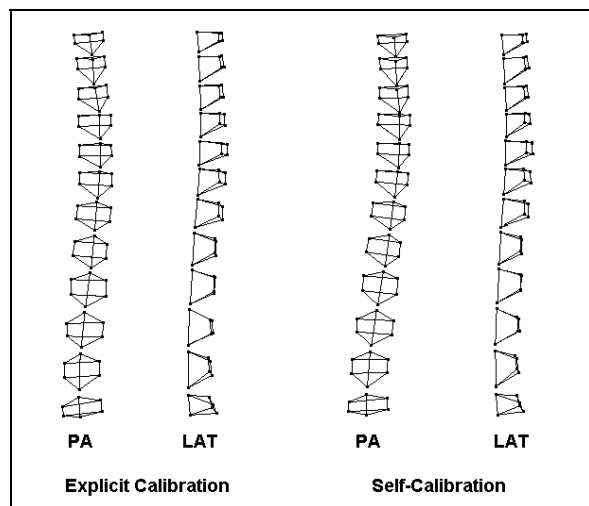


Figure 2: A spine reconstructed by explicit calibration (with a calibration object) and by self-calibration (without calibration object). Postero-anterior (PA) and lateral (LAT) views are presented.

## CONCLUSION

The results of self-calibration are very promising. The accuracy is sufficient for the extraction of meaningful 3D clinical data. This algorithm will allow the 3D reconstruction of spines from intra-operative x-rays in the context of retrospective studies, which is impossible with previous techniques that require a calibration object. Furthermore, this technique will make it easier to undertake vast multi-centre studies since it is compatible with standard radiological procedures.

## REFERENCES

- [1] F. Cheriet *et al.*, Reconstruction radiographique peropératoire de la colonne vertébrale scoliotique, *Annales de chirurgie*, Vol. 53, no. 8, 1999, pp. 808-815.
- [2] F. Cheriet *et al.*, Towards the Self-Calibration of a Multi-view Radiographic Imaging System for the 3D Reconstruction of the Human Spine and Rib Cage, *International Journal of Pattern Recognition and Artificial Intelligence*, Vol. 13, No. 5, 1999, pp. 761-779.
- [3] L. Chen *et al.*, An investigation on the Accuracy of Three-dimensional Space Reconstruction Using the Direct Linear Transform, *Journal of Biomechanics*, Vol. 27, No. 4, Elsevier Science Ltd, Great Britain, 1994, pp. 493-500.
- [4] H. Labelle, *et al.*, "Variability of Geometric Measurements from Three-dimensional Reconstructions of Scoliotic Spines and Rib Cages", *Eur. Spine J.*, Springer-Verlag, 1995, pp. 88-94.
- [5] E. Trucco, A. Verri, *Introductory Techniques for 3-D Computer Vision*, Prentice Hall, Upper Saddle River, New Jersey, 1998, 343 p.
- [6] R. I. Hartley, In Defense of the Eight-Point Algorithm, *IEEE Trans. Pattern Analysis and Machine Intelligence*, Vol. 19, No. 6, 1997, pp. 580-593.
- [7] M. Pollefeys, Tutorial: 3D Modeling from Images, *3<sup>rd</sup> International Conference on 3D Digital Imaging and Modeling*, Québec City, Canada, May 2001, 124 pages.
- [8] J. Novosad, *et al.*, Self-Calibration of Biplanar Radiographs for the Retrospective Comparative Study of the 3D Correction of Adolescent Idiopathic Scoliosis, to appear in: *Research into Spinal Deformities*, IOS Press, 2002.